RECEIVED BY OSTI AUG 06 1985

CONF-850711--12

CONF-850711--12

DE85 015660

By acceptance of this article, the publisher or recipient acknowledges the U.S. Government's right to retain a nonexclusive, royalty-free license in and to any copyright covering the article.

GAMMA AND NEUTRON IRRADIATION TESTS ON COMMERCIAL IC OP AMPS*

Eldredge J. Kennedy,† Alton C. Morris, Jr,** and David K. Su††

Abstract

Experimental results of gamma and neutron irradiation tests on 30 types of integrated-circuit operational amplifiers from 11 manufacturers are presented. All units were low-cost, commercial-grade devices. Op amps were evaluated for changes in offset voltage, input bias current, power supply current, open-loop gain, gain-bandwidth product, slew rate, power-supply and common-mode rejection ratios. Bipolar transistor op amps with resistive collector load resistors for the input stage indicated the best radiation hardness.

DISCLAIMER

This report was prepared as an account of work sponsored by an agency of the United States Government. Neither the United States Government nor any agency thereof, nor any of their employees, makes any warranty, express or implied, or assumes any legal liability or responsibility for the accuracy, completeness, or usefulness of any information, apparatus, product, or process disclosed, or represents that its use would not infringe privately owned rights. Reference herein to any specific commercial product, process, or service by trade name, trademark, manufacturer, or otherwise does not necessarily constitute or imply its endorsement, recommendation, or favoring by the United States Government or any agency thereof. The views and opinions of authors expressed herein do not necessarily state or reflect those of the United States Government or any agency thereof.

---

*Research sponsored by the Office of Spent Fuel Management and Reprocessing Systems, performed at Oak Ridge National Laboratory operated by Martin Marietta Energy Systems, Inc., for the U.S. Department of Energy, under Contract No. DE-AC05-84OR21400.

†Electrical Engineering Department, University of Tennessee, Knoxville, TN 37996-2100 and Oak Ridge National Laboratory (part-time) Oak Ridge, TN 37831.

**Oak Ridge National Laboratory, Oak Ridge, TN 37831.

††Formerly University of Tennessee, Knoxville. Now employed by Hewlett Packard Corp, Corvalis, Oregon.

DISTRIBUTION OF THIS DOCUMENT IS UNLIMITED

Introduction

Radiation-tolerant components comprise two basic categories; (1) those designed specifically for radiation hardness and marketed especially for the military with full MIL-Spec. processing and (2) those standard commercial components that are radiation hard because of inherent design and fabrication processes. Components in the first category are limited and costly; hence, the goal of this testing program has been to identify less expensive alternatives among standard commercially available parts. Since the ultimate intended use of the parts is in control systems for radiation hot cell applications that have expected temperature environments of 10 to 50°C and a component lifetime of one to three years, the full MIL-Spec. processing was not essential.

The goal of this research was to identify radiation-hard integrated circuits that could withstand a total gamma dose of 1 Mrad and a total neutron dose of 10^{13} n/cm^2. The gamma rate effect was negligible since the maximum anticipated dose rate was 10^5 rad/h (28 r/s).

Although several categories of integrated circuits and devices were tested for radiation hardness, this paper concentrates on parameter changes in various operational amplifiers (op amps) produced by gamma and neutron irradiation. Gamma radiation was obtained using a Gammacell 200 Cobalt-60 source, with an average dose rate of 6.3×10^4 rad/h. Devices were checked at 1-Mrad intervals up to a maximum dose of 4 Mrad. The same devices were then subjected to a thermal neutron flux of 5×10^{11} n/cm^2/s for 100 s in the Bulk Shielding Reactor at the Oak Ridge National Laboratory (ORNL). The additional gamma dose accumulated during the neutron irradiation was approximately 16 krad. All devices were irradiated with shorted leads at zero bias. Table 1 shows the 30 types of op amps from 11 manufacturers tested. Program time and cost constraints limited the sample size that varied from four to six units per op amp. Typically, at least two different date codes were included in each device set. For those op amps that indicated significant hardness, additional testing with more units will be carried out later.

DC measurements were made using the Tektronix 577 curve tracer, with a Model 178 linear IC test fixture. Slew rate and gain-bandwidth product were evaluated using high-frequency test fixtures driven by either square-wave or sinusoidal signals.

Results

All op amps were evaluated for changes in offset voltage (V_{OS}), input bias current (I_B), power-supply current (I_S), open-loop gain (A_{OL}), gain-bandwidth product (GB), power-supply rejection ratio (PSRR), and common-mode rejection ratio (CMRR). Shown in Figs. 1 through 9 are the average observed changes in several of the parameters. Worst-case

radiation effects observed on any unit of each type tested are summarized in Table 2.

One of the most significant dc parameters of interest in an op amp is the V_{OS}. It was observed that those op amps having bipolar transistor input stages with collector load resistors (as opposed to active current sources for the load) gave the least change in V_{OS} with radiation. Op amps in this category were the OP27, OP37, and NE5534 (and the dual NE5532). Figures 1 and 3 show that these unit types indeed have negligible V_{OS} changes as compared with most other bipolar input devices, and certainly much less change than any junction field-effect transistor (JFET) input op amp, as shown in Fig. 2.

The Appendix shows that, using qualitative reasoning, one could anticipate the offset voltage change of a differential-input bipolar stage to be a factor of 80 less than that of a similar JFET input stage design. Similarly, the change in V_{OS} with radiation for a bipolar input stage with resistive collector load resistors could be expected to be significantly less than the V_{OS} change for bipolar stages having active (current-mirror type) loads.

Since considerable neutron-induced beta and gamma radiation was emitted from the op amps after neutron irradiation, the devices had to be stored for five days until the radiation decayed to a safe level for testing, thus the final data points on these figures of neutron irradiation include some room-temperature annealing effects.

It is also apparent from Figs. 1 through 3 that those bipolar input op amps with dielectric isolation (HA2505, HA2525, HA2625) had small changes in V_{OS} after radiation.

In general, the most significant parameter affected by radiation was the input bias current, I_B, as shown in Figs. 4 and 5. The increase of I_B for JFET input op amps was typically two orders of magnitude, and a saturation effect occurred at more than 1 Mrad. These increases are probably caused by surface effects at the reverse-biased gate-to-channel junctions. Even though the input current increased by a factor of 20, the OPA111 op amp had the smallest value of I_B after 3 Mrads, having a typical value of less than 200 pA. The changes in I_B for most bipolar input op amps also tended to saturate after 1 Mrad, although some devices employing pnp lateral transistors in an input bias current cancellation network (such as the OP27) indicated saturation beyond this value. The OP27 devices from Precision Monolithics (PMI) indicated much less increase of I_B than did OP27 op amps from Micro Power Systems. The dielectrically isolated HA2625 and HA5135 units as well as the OP27 (PMI) units had the lowest values of I_B after 2 Mrads than any other bipolar op amp.

Figures 6 and 7 indicate the decrease of A_{OL} with radiation. For most general-purpose op amps, A_{OL} was still greater than 80 dB after 2 Mrads, and the OP27 and OP37 op amps indicated values of A_{OL} greater than 110 dB even after 4 Mrads. Power supply currents of all op amps decreased after irradiation. Devices that had less than a 15% change in

I_S were the OP17, OP27 (PMI), OP37, OPA111, HA2505, HA2525, HA2539, HA2540, HA2635, HA4640, and HA5084. The change in power supply current appeared to be a strong function of not only the internal biasing network used, but also of whether the op amp employed dielectric isolation (as do most of the Harris devices) or not. Dielectrically isolated op amps generally had less change in power supply currents than the others.

The gain-bandwith product change with radiation is shown in Figs. 8 and 9. For a typical op amp, the gain-bandwidth product is related to the input stage transconductance g_{mi} and the dominant pole capacitance C_f as

$$GB = \frac{g_{mi}}{2\pi\ C_f} \quad . \tag{1}$$

Further, the slew rate for most general-purpose op amps is determined by the input stage current source I_i and the capacitance C_f, or

$$SR = \frac{I_i}{C_f} = \left(\frac{2\pi I_i}{g_{mi}}\right) GB \quad . \tag{2}$$

Since a decrease in power supply current should relate to a decrease in both g_{mi} and I_i, then from Eqs. (1) and (2) the decrease in power supply current should relate correspondingly to a decrease in both GB and SR.

Conclusions

For a general-purpose, low-V_{OS} requirement, the OP27 and OP37 devices offer the best choice of those op amps tested for a radiation environment of less than 4 Mrads and 10^{13} n/cm^2. Unfortunately, the increase in I_B restricts the use of these devices to those circuit applications that can operate with I_B values to 0.5 μA; however, the offset current did remain less than 10% of I_B for all OP27-OP37 devices tested. For high-frequency applications (where changes in I_B are usually not so important), the HA2539-HA2540 op amps, having post-irradiation values of GB and SR greater than 200 MHz and 200 V/μs respectively, should prove useful. Similarly, the other dielectrically isolated units, the HA2505, HA2525, and HA2625 offer small V_{OS} changes, with an increase in I_B in all units tested to values ≤ 1 μA. The NE5534 and the NE5532 dual units have insignificant V_{OS} changes, but I_B increases to greater than 1 μA. Unfortunately, no FET input op amp tested provided a sufficiently small change in V_{OS} to be useful in circuits with dc gains greater than 10. Table 2 summarizes the

worst-case changes observed and subjectively categorizes the op amps tested.

Acknowledgments

The authors wish to express their appreciation to the Consolidated Fuel Reprocessing Program (CFRP) at the Oak Ridge National Laboratory for providing funding and incentive for this research effort.

Appendix

First, let us compare the changes in V_{OS} caused by gamma irradiation for a bipolar transistor differential input stage as opposed to a JFET transistor differential input stage. The offset voltage for two bipolar input transistors, Q_1 and Q_2, connected as a single differential stage with collector load resistors R_1 and R_2 is

$$V_{OS} = V_{BE1} - V_{BE2} \tag{3}$$

where (ignoring any Early effects) the base-emitter potential V_{BE} is related to the collector current I_C by[2]

$$I_C = I_S \exp (V_{BE}/V_T) \tag{4}$$

where V_T = the thermal potential = kT/q, and I_S is the reverse saturation current. Hence, substituting Eq. (4) into Eq. (3) gives

$$V_{OS} = V_T \ \ln \frac{I_{C1}}{I_{C2}} + \ln \frac{I_{S1}}{I_{S2}} \tag{5}$$

Now, make the following assumptions

$$\Delta I_c = I_{C1} - I_{C2}, \quad I_c = \frac{I_{C1} + I_{C2}}{2} \ ,$$

$$\Delta I_s = I_{S1} - I_{S2}, \quad I_s = \frac{I_{S1} + I_{S2}}{2} \ . \tag{6}$$

Thus, we have

$$I_{C1} = I_c + \frac{\Delta I_c}{2} , \ I_{C2} = I_c - \frac{\Delta I_c}{2} \ ,$$

$$I_{S1} = I_s + \frac{\Delta I_s}{2}, \quad I_{S2} = I_s - \frac{\Delta I_s}{2} \quad . \tag{7}$$

Further, by noting that $\Delta I_C << I_C$ and $\Delta I_S << I_S$ for a good differential design, then by substitution and a Taylor's series expansion we obtain

$$V_{OS} \text{ (bipolar stage)} \approx V_T \left(\frac{\Delta I_c}{I_c} - \frac{\Delta I_s}{I_s} \right) . \tag{8}$$

Thus, the input offset voltage is a function of the mismatch in collector currents as well as I_S, which involves physical device parameters such as base-doping concentration, base width, collector-doping concentration, and base-emitter area.

For the present, let us ignore load effects in Eq. (8), and concentrate on changes in offset voltage caused by differences in transistor parameters. Then the offset voltage due to transistor device parameters reduces to

$$\left| V_{OS} \right| \approx V_T \left| \frac{\Delta I_s}{I_s} \right| \tag{9}$$

For a graded-base transistor, the saturation current I_S is given by (see ref. 2):

$$I_s = \left(\frac{q \; D_n \; n_i^2}{Q_B} \right) A_{EB} \; , \tag{10}$$

where D_n is the mean electron diffusivity, n_i is the intrinsic carrier concentration, Q_B is the total charge in the base, and A_{EB} is the base-emitter area. For simplicity, assume a square base-emitter area of d^2, thus Eq. (10) can be written as

$$I_s = \left(\frac{q \; D_n \; n_i^2}{Q_B} \right) d^2 \quad . \tag{11}$$

The primary effect of ionizing radiation is the buildup of trapped charges and interface states. These trapped charges in the oxide will alter the shape of the emitter, base, and collector[3] by attracting electrons to the p-n junction under the oxide. Thus, one of the dominant changes in I_S is due to the change in the base-emitter area. Hence, from Eq. (11) we can obtain

$$\delta I_s = 2\left(\frac{q\, D_n\, n_i^2}{Q_B}\right) d \times \delta d \quad , \tag{12}$$

where δ refers to the change in the parameter <u>due to irradiation</u>; whereas the symbol Δ referred to the <u>mismatch</u> in the two transistors. By reduction, from Eq. (12) we therefore obtain

$$\frac{\delta I_s}{I_s} = 2\left(\frac{\delta d}{d}\right). \tag{13}$$

If the two transistors Q_1 and Q_2 were perfectly matched prior to irradiation, then, from Eq. (8), the initial offset voltage and the initial mismatch in I_S would be zero. Thus, if I_S of one transistor were changed by δI_S after irradiation ($\delta I_S \ll I_S$), then the mismatch in I_S becomes

$$\Delta I_S \text{ (after irradiation) } = \delta I_S \;,$$

and thus from Eq. (9) we have that

$$V_{OS} \text{ (after irradiation) } = V_T \left| \frac{\delta I_s}{I_s} \right| \quad . \tag{14}$$

Hence, we finally obtain using Eqs. (13) and (14), at 25°C,

$$\boxed{\delta\, V_{OS} \text{ (bipolar stage) } \approx 0.052 \left(\frac{\delta d}{d}\right).} \tag{15}$$

For a JFET differential input stage with two matched JFETs, J1 and J2, the offset voltage is the difference of the two gate-source voltages, or

$$V_{OS} \text{ (JFET) } = V_{GS_1} - V_{GS_2} \quad . \tag{16}$$

Assuming square-law characteristics for the JFETs, the gate-source voltage is related to the pinch-off voltage V_p, the drain current I_D, and the zero-bias drain saturation current I_{DSS} by

$$V_{GS} = V_p \left[1 - (I_D/I_{DSS})^{1/2}\right] . \tag{17}$$

Using similar assumptions as for the bipolar circuit, Eqs. (6) and (7), one obtains

$$V_{OS} = \Delta V_p - V_p \left(\frac{I_D}{I_{DSS}}\right)^{1/2} \left(\frac{\Delta I_D}{2I_D} - \frac{\Delta I_{DSS}}{2I_{DSS}} + \frac{\Delta V_p}{V_p}\right) . \qquad (18)$$

For most JFET designs in monolithic op amps, the drain current is much less than I_{DSS}, hence the second term in Eq. (18) is small so that $V_{OS} \approx \Delta V_p$ in Eq. (18).

If we approximate the gate and channel by an abrupt junction, then the pinch-off voltage, (V_p), is related by[4]

$$V_p = \left(\frac{q\ N_D}{8\varepsilon}\ a^2 - \psi_o\right) , \qquad (19)$$

where a is the zero-bias channel thickness, N_D is the channel doping concentration, ε is the permittivity of free space, q is the charge of an electron, and ψ_o is the built-in barrier voltage of the gate-channel junction.

Since the buildup of positive charge due to ionizing radiation will affect the zero-bias channel thickness a, then from the above equations

$$\delta V_p = \left(\frac{2q\ N_D a}{8\varepsilon}\right) \delta a \qquad (20)$$

or

$$\delta V_p = 2\ (V_p + \psi_o)\ \frac{\delta a}{a} \ . \qquad (21)$$

By similar arguments, assuming perfect matching before irradiation as for the bipolar stage, the change in offset voltage reduces to

$$\delta V_{OS}\ \text{(JFET stage)} \approx 2\ (V_p + \psi_o)\ \frac{\delta a}{a} \ . \qquad (22)$$

A typical value for a bipolar-FET process is $V_p + \psi_o \approx 2V$. Thus, for a standard JFET input stage a reasonable approximation for changes in V_{OS} due to ionizing radiation is

$$\boxed{\delta V_{OS} \text{ (JFET stage)} \approx 4\left(\frac{\delta a}{a}\right).} \tag{23}$$

Finally, let us compare the changes in offset voltage produced by ionizing radiation for bipolar transistor input stages with and without active transistor loads. The equation for the offset voltage for a bipolar transistor input stage was derived earlier as Eq. (8). The component of offset resulting from the collector load is the first part, or

$$\left|V_{OS}\right| \approx V_T \left|\frac{\Delta I_c}{I_c}\right| . \tag{24}$$

Assuming resistive collector load resistors R_1 and R_2 with identical voltage drops, then $I_{C1}R_1 = I_{C2}R_2$. By definition, as previously,

$$R_1 = R + \frac{\Delta R}{2}, \; R_2 = R - \frac{\Delta R}{2},$$

$$I_{C1} = I_c + \frac{\Delta I_c}{2}, \; I_{C2} = I_c - \frac{\Delta I_c}{2}, \tag{25}$$

and simplifying we obtain

$$\frac{\Delta I_c}{I_c} \approx \frac{\Delta R}{R}, \tag{26}$$

or due to the resistive loads, using Eq. (24)

$$V_{OS} \approx V_T \left(\frac{\Delta R}{R}\right). \tag{27}$$

In a monolithic integrated circuit operational amplifier, a resistor is determined by the sheet resistivity, $R_{\square}$ (specified in ohms per square), and the length-to-width ratio of the resistor, L/W. Thus, a collector resistor value is given by

$$R = \left|\frac{L}{W}\right| R_{\square} . \tag{28}$$

Both length L and width W are surface parameters that change with positive trapped charges in the oxide. The changes are probably correlated since positive trapped charges in the oxide should cause both the length L and width W of a p-type diffused resistor to decrease by attracting electrons to the p-n junction beneath the oxide. The sheet

resistivity ($R_\square$) is a nonlinear function of the doping and junction depth. Unlike the length and width of the resistor, both the doping and the junction depth are bulk parameters and probably weak functions of surface damages caused by ionization at low dose rates. Therefore, the sheet resistivity is not expected to change significantly with ionizing radiations. The change in resistance after irradiation could thus be reasonably stated as

$$\delta R = R_\square \left(\frac{W\delta L - L\delta W}{W^2} \right) \tag{29}$$

or from Eqs. (28) and (29),

$$\frac{\delta R}{R} = \frac{\delta L}{L} - \frac{\delta W}{W} \quad . \tag{30}$$

If the two collector resistors were perfectly matched with $\Delta R = 0$ before irradiation, and then one of the resistors changed by δR, we use Eq. (27) to calculate the change in offset voltage due to resistive collector loads as

$$\delta\, V_{OS} = V_T \left(\frac{\delta R}{R} \right) \tag{31}$$

or we obtain for a resistive load at room temperature,

$$\boxed{\delta\, V_{OS} \text{ (resistive load)} = 0.026 \quad \frac{\delta L}{L} - \frac{\delta W}{W} \quad .} \tag{32}$$

For a simple, active load configuration comprising input bipolar transistors Q_1 and Q_2 with a current-mirror load of bipolar transistors Q_3 and Q_4, the base-emitter voltage of the current-mirror transistors are equal, or

$$V_{BE_3} = V_{BE_4} \quad . \tag{33}$$

Using Eq. (4), we obtain the ratio

$$\frac{I_{C3}}{I_{C4}} = \frac{I_{S3}}{I_{S4}} \quad . \tag{34}$$

Assuming $h_{FE} >> 1$, then $I_{C1} \approx I_{C3}$, and $I_{C2} \approx I_{C4}$. Now, define the average value of I_{S3} and I_{S4} as I_{SL}, where

$$I_{SL} = \frac{I_{S3} + I_{S4}}{2} \quad , \tag{35}$$

and then $\Delta I_{SL} = I_{S3} - I_{S4}$, or

$$I_{S3} = I_{SL} + \frac{\Delta I_{SL}}{2}$$

$$I_{S4} = I_{SL} - \frac{\Delta I_{SL}}{2} \quad . \tag{36}$$

Then

$$\frac{\Delta I_c}{I_c} = \frac{\Delta I_{SL}}{I_{SL}} \quad , \tag{37}$$

or from Eqs. (37) and (24)

$$V_{OS} \approx V_T \left(\frac{\Delta I_{SL}}{I_{SL}}\right) . \tag{38}$$

The value of I_S is a function of the base-emitter junction area, as shown earlier in Eq. (10). For a junction length L_E and width W_E, taking approximate changes in Eq. (38) gives

$$\frac{\delta I_S}{I_S} = \frac{\delta L_E}{L_E} + \frac{\delta W_E}{W_E} \quad ,$$

or finally from Eq. (38)

$$\delta V_{OS} \text{ (active load)} \approx 0.026 \left(\frac{\delta L_E}{L_E} + \frac{\delta W_E}{W_E}\right) \quad . \tag{39}$$

Let us compare the results of Eqs. (32) and (39). First, changes in the lengths and widths should be correlated. That is, they should be either both increasing or both decreasing. Assuming the same order of magnitude change in the dimensions, the change in offset voltage due to a resistive load would be smaller because of the possible cancellation effect of the relative changes in its length and width. Secondly, the dimension of a typical resistor is much larger than that of the base-emitter junction. Smaller relative changes in length and width for the resistive load would therefore be expected.

References

1. J. A. Harrell, P. L. Manke, and J. E. Gover, "The Application of Remote Electronics in a Nuclear Fuel Reprocessing Environment: Radiation Effects and Design Guidelines," Sandia National Laboratory Report SAND82-2151, January 1983.

2. P. R. Gray and R. G. Meyer, Analysis and Design of Analog Integrated Circuits, 2nd ed., New York, John Wiley & Sons, 1984.

3. D. K. Nichols, "A Review of Dose Rate Dependent Effects of Total Ionizing Dose (TID) Irradiations," IEEE Tran. Nucl. Sci., Vol. NS-27, No. 2, April 1980.

4. A. S. Grove, Physics and Technology of Semiconductor Devices, New York, John Wiley & Sons, 1967.

5. D. K. Su, "The Effects of Gamma and Neutron Irradiations on Linear Integrated Circuits and Power Devices," Master of Science Thesis, The University of Tennessee, Knoxville, March, 1985 (to be published as an Oak Ridge National Laboratory TM Report).

Captions

Table 1. Operational amplifiers tested

Table 2. Subjective summary of test results for op amps

Fig. 1. Average offset voltage versus radiation dose for bipolar input op amps.

Fig. 2. Average offset voltage versus radiation dose for JFET input op amps.

Fig. 3. Average offset voltage versus radiation dose for dual and quad op amps.

Fig. 4. Input bias current versus radiation dose for JFET input op amps.

Fig. 5. Input bias current versus radiation dose for bipolar input op amps.

Fig. 6. Open-loop gain versus radiation dose for op amps with low initial gain.

Fig. 7. Open-loop gain versus radiation dose for op amps with high initial gain.

Fig. 8. Gain-bandwidth product versus radiation dose for op amps having GB <5 MHz after irradiation.

Fig. 9. Gain-bandwidth product versus radiation dose for op amps having GB >5 MHz after irradiation.

Table 1. Operational amplifiers tested

Device (manufacturer)	Description
CA3140 (RCA)	MOSFET input(BiMOS); 4.5 MHz GB
HA2505 (Harris)	Bipolar; 12 MHz GB; dielectric isolation
HA2525 (Harris)	Bipolar; 20 MHz GB; dielectric isolation; Av ≥3
HA2539 (Harris)	Bipolar; 600 MHz GB; dielectric isolation; Av ≥10
HA2540 (Harris)	Bipolar, 400 MHz GB; dielectric isolation; Av ≥10
HA2625 (Harris)	Bipolar, 100 MHz GB; dielectric isolation; Av ≥5
HA4156 (Harris)	Quad; bipolar; junction isolation; 4 MHz GB; 741-type op amp.
HA4640 (Harris)	Quad; bipolar; dielectric isolation; high temp (>250°C)
HA5084 (Harris)	Quad; JFET input(BiFET); dielectric isolation; 4 MHz GB
HA5135 (Harris)	Bipolar; Superbeta input; precision; 2.5 MHz GB; dielectric isolation
ICL7621 (Intersil)	Dual; low-power CMOS
LF351 (National)	JFET input(BiFET); general purpose; 4 MHz GB
LF353 (National)	Dual; JFET input(BiFET); general purpose; 4 MHz GB
LT1012 (Linear Tech)	Bipolar; low-power
LT1037 (Linear Tech)	Bipolar; low-noise; precision; Av ≥5
NE5532 (Signetics)	Dual; bipolar; low-noise op amp.
NE5534 (Signetics)	Bipolar; low-noise; general purpose; Av ≥5
OP11 (PMI)	Quad; bipolar; 741-type; general purpose
OP15 (PMI)	JFET input(BiFET); general purpose; 6 MHz GB
OP16 (PMI)	JFET input(BiFET); general purpose; 8 MHz GB
OP17 (PMI)	JFET input(BiFET); 30 MHz GB; Av ≥5
OP22 (PMI)	Bipolar; programmable; low-power; single or dual power supplies
OP27 (MPS)	Bipolar; precision; low-noise; 8 MHz GB
OP27 (PMI)	Bipolar; precision; low-noise; 8 MHz GB
OP32 (PMI)	Bipolar; programmable; low-power; single or dual power supplies; Av ≥10
OP37 (PMI)	Bipolar; precision; low-noise; 63 MHz GB; Av ≥5
OP215 (PMI)	Dual; JFET input(BiFET); general purpose; 6 MHz GB
OPA111 (Burr Brown)	JFET; precision; low-noise; $I_B<1$pA; dielectric isolation
OP227 (PMI)	Dual; bipolar; precision; low-noise; 8 MHz GB
TLC251 (Texas Instr)	CMOS
1344 (Philbrick)	JFET input(BiFET); 100 MHz GB; dielectric isolation; Av ≥10

Table 2. Subjective summary of test results for op amps

Device (manufacturer)	Total gamma (Mrad)	Total neutron ($\times 10^{13}$ n/cm^2)	Worst-case radiation effects observed on any unit
		Group I. Recommended	
OP27 (PMI)	4	5	Input current of 140 nA, GB decrease of 20%.
OP37 (PMI)	3	5	Input current of 500 nA, GB decrease of 20%.
HA2505 (HAR)	2	5	Input current of 500 nA, open-loop gain of 80 dB.
HA2525 (HAR)	2	5	Input current of 1 μA, open-loop gain of 74 dB.
HA2625 (HAR)	2	5	Input current of 113 nA, GB decrease of 20%.
HA2539 (HAR)	2	5	Input current of 21 μA, open-loop gain of 79 dB.
HA2540 (HAR)	2	5	Input current of 23 μA, open-loop gain of 70 dB.
HA4640 (HAR)	2	5	Input current of 10 μA, reduction in drive of 2 KΩ load.
		Group II. Usable	
HA5135 (HAR)	2	5	Input offset voltage of 0.6 mV and input current of 100 nA. GB decrease of 30%.
OP227 (PMI)	2		Input current of 2 μA GB and SR decrease of 50%.
NE5532 (SIG)	2		Input current of 4 μA.
NE5534 (SIG)	2	5	Input current of 7.4 μA.
OP27 (MPS)	4	5	Input current of 0.8 μA.
HA4156 (HAR)	2		Input offset voltage of 4 mV, input current of 3 μA. Decreased drive with 2-KΩ load. GB decrease of 50%
OP17 (PMI)	2	5	Input offset voltage of 15 mV, input current of 1 nA. SR increases. PS current decreases 20%.
OP11 (PMI)	2	5	Input offset voltage of 3 mV, input current of 3 μA. SR and GB decrease of 70%.
		Group III. Not Recommended	
LF353 (NAT)	2	5	Input offset voltage of 5 mV, large reduction in output drive of one unit, input current of 5 nA.
OP15 (PMI)	4	5	Input offset voltage of 40 mV, input current of 2 nA. PS current decrease of 60%.
OPA111 (BB)	3	5	Input offset voltage of 50 mV, input current of 300 pA.
1344 (TEL)	3	5	Input offset voltage of 20 mV, input current of 1 nA. Decrease in output drive.
HA5084 (HAR)	2	5	Input offset voltage of 85 mV, input current of 1.3 nA.
OP215 (PMI)	3	5	Input offset voltage of 65 mV with no correlation between devices on the same chip, input current of 1.6 nA.
OP16 (PMI)	2	5	Input offset voltage of 170 mV, input current of 3 nA. PS current decrease of 70%.
OP22 (PMI)	2	5	Not functional for 20-MΩ set resistor. Drastic reduction in drive, slew rate, GB.
OP32 (PMI)	2	5	Not functional for 20-MΩ set resistor. Drastic reduction in drive, slew rate, GB.
		Group IV. Failed	
LF351 (NAT)	2	5	Input offset voltage of 840 mV and drifted by 100 mV during power-on after irradiation.
TLC251 (TI)	2		Input offset voltage drifted wildly. Drastic reduction in output drive.
CA3140 (RCA)	1		Failed.
ICL7621 (INT)	1		Failed.
LT1012 (LT)	1		Failed.
LT1037 (LT)	1		Failed.

ORNL-DWG 85C-13171

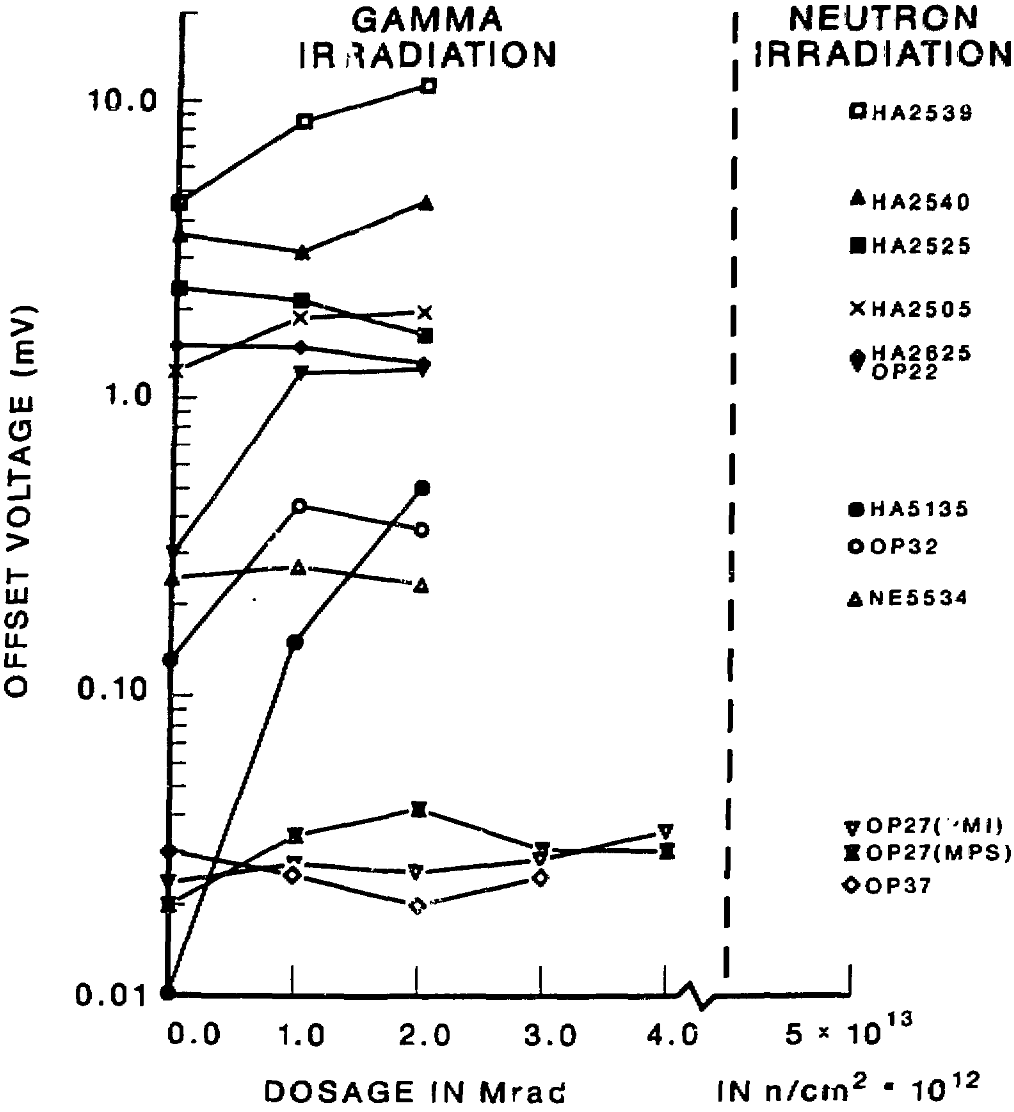

ORNL-DWG 85C-13174

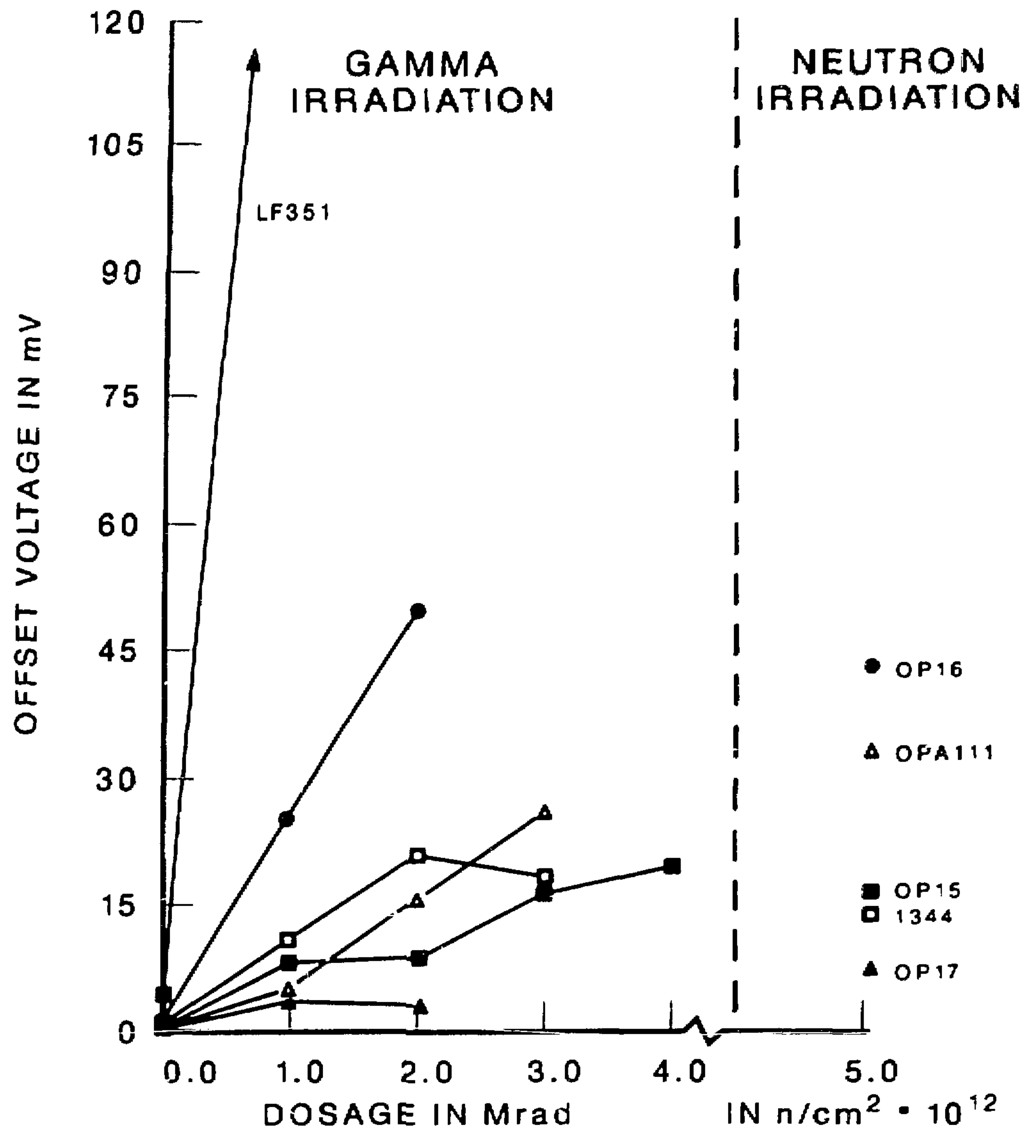

ORNL-DWG 85C-13175

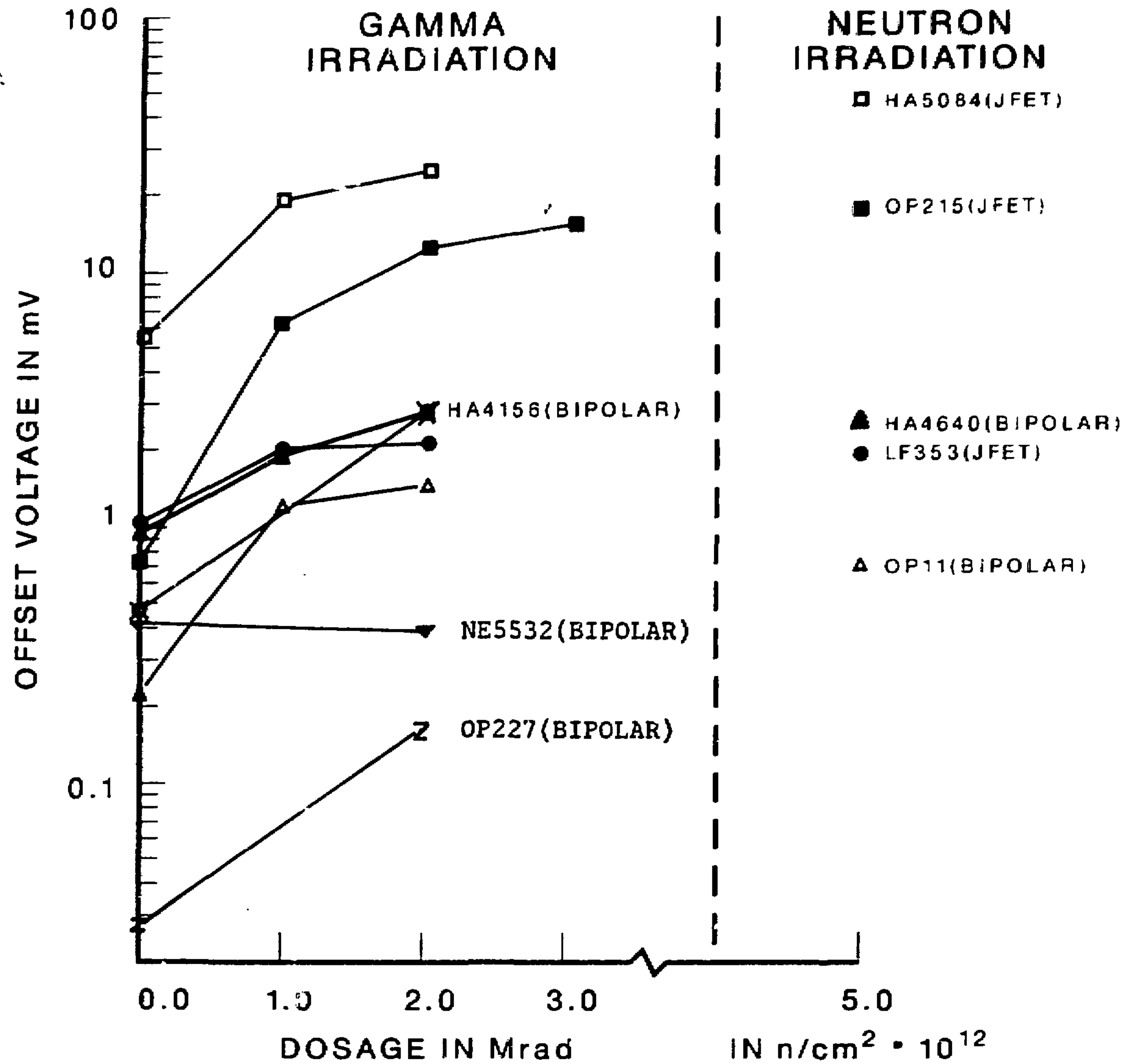

ORNL-DWG 85C-13173

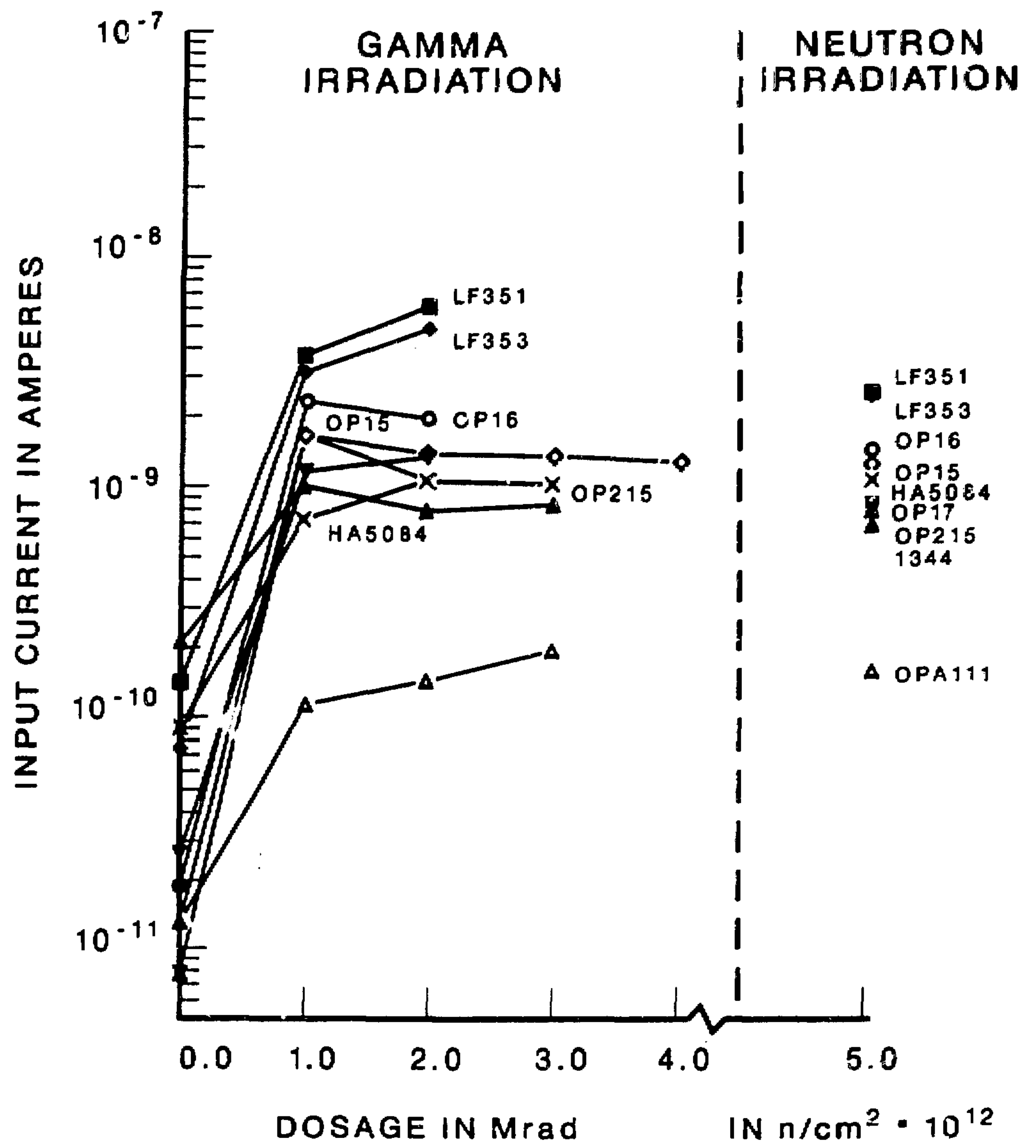

ORNL-DWG 85C-13172

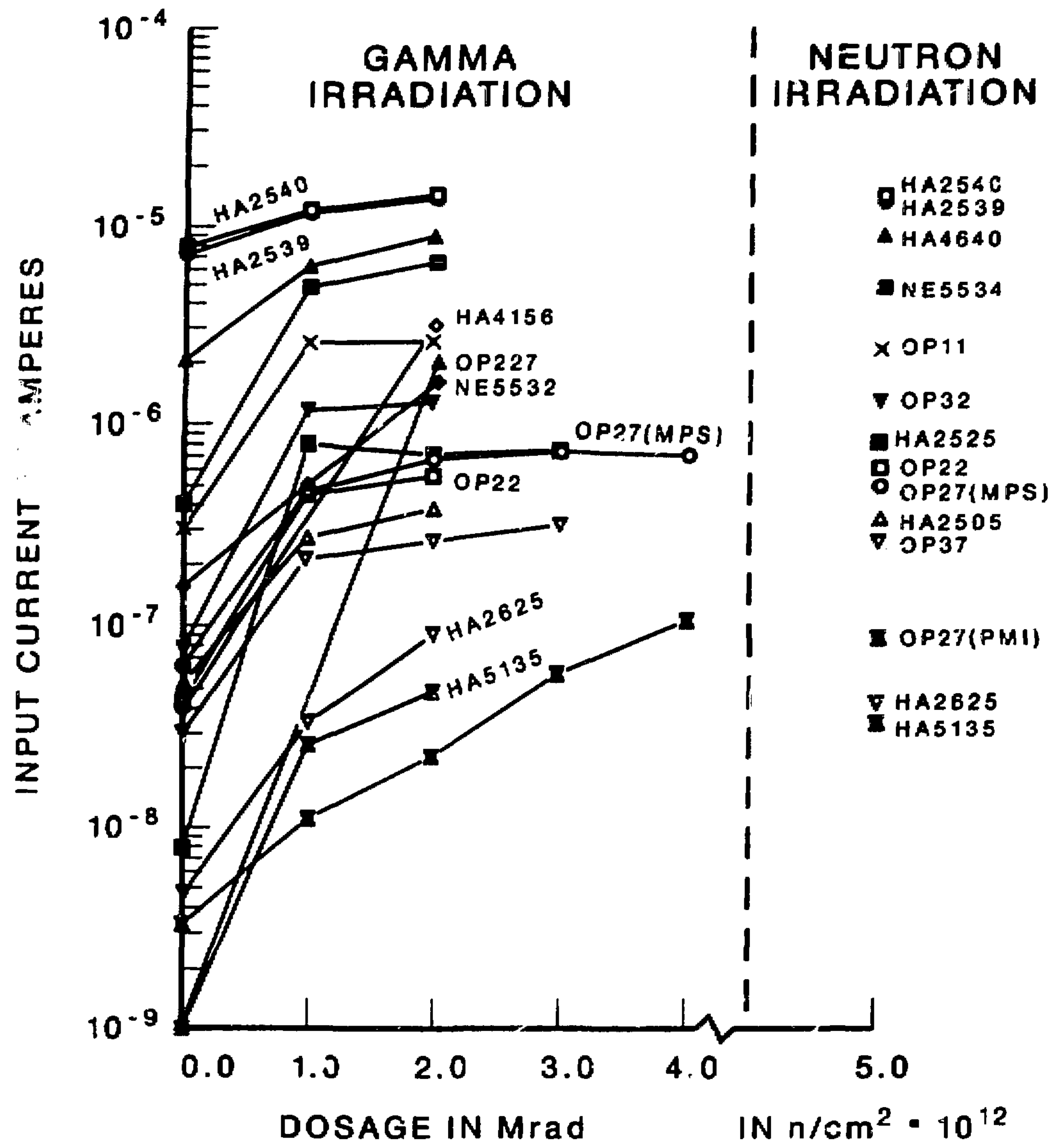

ORNL-DWG 85C-13177

GAMMA IRRADIATION

NEUTRON IRRADIATION

OPEN-LOOP GAIN IN dB

129
122
115
108
101
94
87
80
73

0.0 1.0 2.0 3.0 4.0 5.0

DOSAGE IN Mrad

IN n/cm^2 • 10^{12}

HA2505

▲ OP11
■ OP16
□ OP32
◆ HA4640
× 1344
● OP22
△ HA2540
○ HS2505
◇ HA2539
▽ HA2525

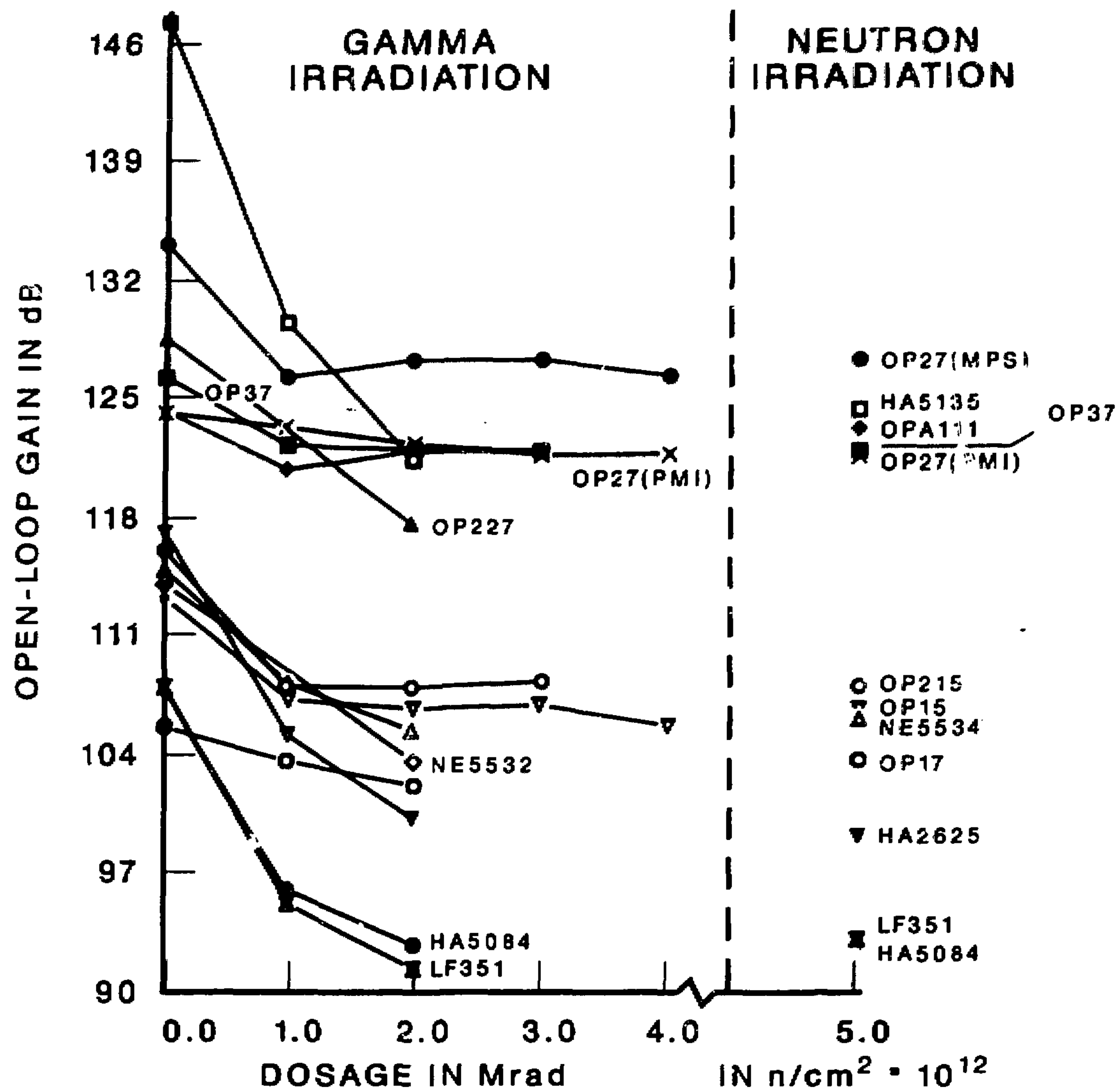
GAMMA IRRADIATION
NEUTRON IRRADIATION
OPEN-LOOP GAIN IN dB
146
139
132
125
118
111
104
97
90
0.0
1.0
2.0
3.0
4.0
5.0
DOSAGE IN Mrad
IN n/cm² • 10¹²
OP37
OP27(PMI)
OP227
NE5532
HA5084
LF351
OP27(MPS)
HA5135
OPA111
OP37
OP27(PMI)
OP215
OP15
NE5534
OP17
HA2625
LF351
HA5084

ORNL-DWG 85- 13178

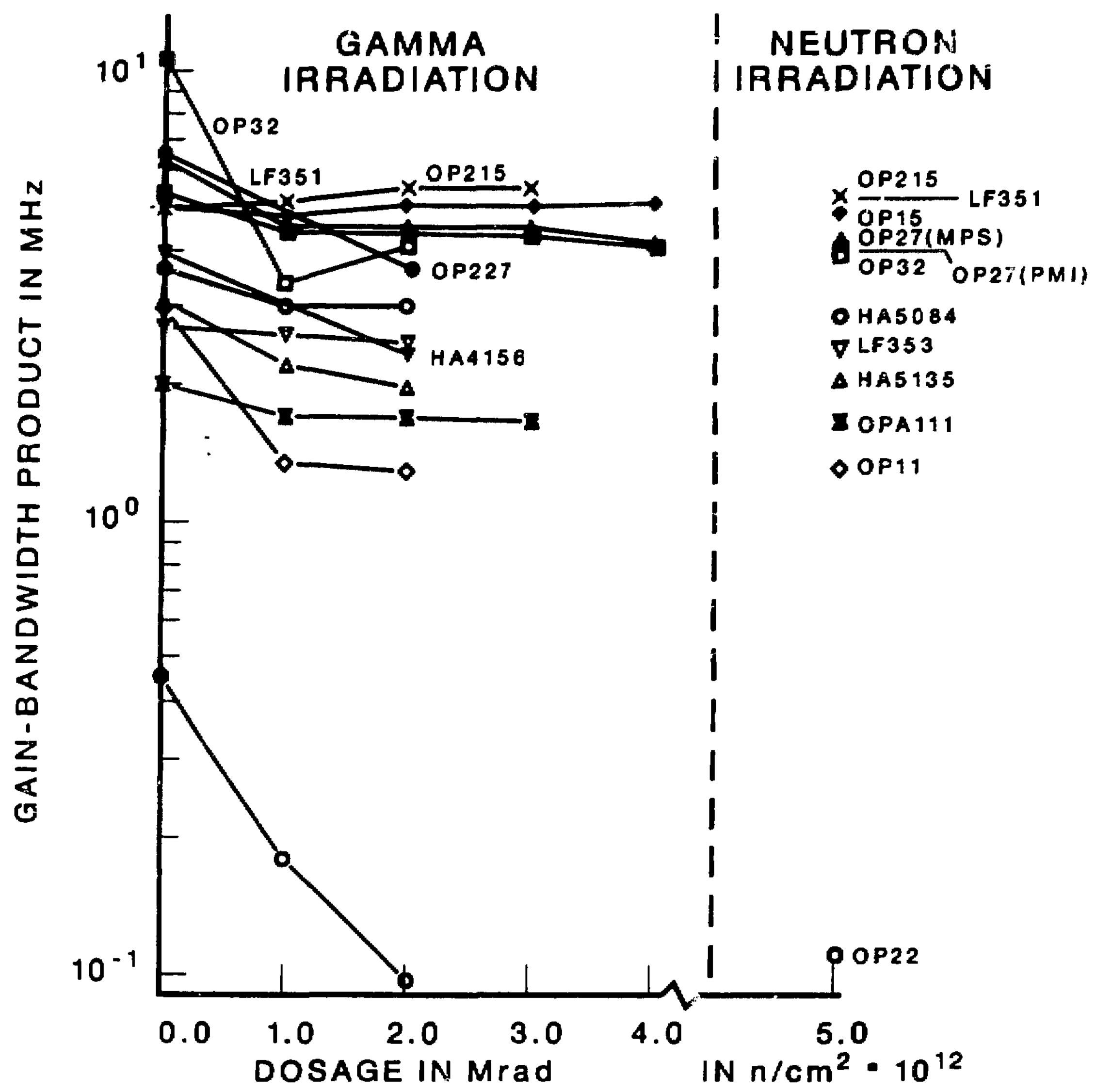

ORNL-DWG 85C-13176

GAMMA IRRADIATION

NEUTRON IRRADIATION

GAIN-BANDWIDTH PRODUCT IN MHz

10^2

10^1

HA2539

HA2540

NE5534

OP37

HA2625

NE5532

OP17

HA4640

HA2525

HA2505

OP16

0.0 1.0 2.0 3.0 4.0 5.0

DOSAGE IN Mrad

IN $n/cm^2 \cdot 10^{12}$

Abstract

Experimental results of gamma and neutron irradiation tests on 30 types of integrated-circuit operational mplifiers (op amps) from 11 manfacturers are presented. All units were low-cost, commercial-grade devices. ›p amps were evaluated for changes in offset voltage, input bias current, power supply current, open-loop ain, gain-bandwidth product, slew rate, and power-supply and common-mode rejection ratios.

Introduction

Although several categories of integrated circuits and devices were tested for radiation hardness, this aper concentrates on parameter changes in various operational amplifiers (op amps) produced by gamma and eutron irradiation. Gamma radiation was obtained using a Gammacell 200 Cobalt-60 source with an average ose rate of 6.3×10^4 rad/h. Devices were checked at 1-Mrad intervals up to a maximum dose of 4 Mrads. he same devices were then subjected to a neutron irradiation dose of 5×10^{13} n/cm^2 in the Bulk Shielding eactor at the Oak Ridge National Laboratory. All devices were irradiated under short lead–zero bias condi-ons. Table 1 shows the 30 types of op amps from 11 manufacturers that were tested. Program time and cost onstraints limited the sample size, which typically ranged from four to six units per op amp. For those op mps that indicated significant hardness, additional testing with more units will be carried out later.

Dc measurements were made using the Tektronix 577 curve tracer with a Model 178 linear IC text fixture. lew rate and gain-bandwidth product were evaluated using high-frequency test fixtures driven by either quare-wave or sinusoidal signals.

Direct-current measurements were made using the Tektronix 577 curve tracer with a Model 178 linear IC ext fixture. Slew rate and gain-bandwidth product were evaluated using high-frequency test fixtures driven by ither square-wave or sinusoidal signals.

Results

Of special interest was the discovery that the radiation-caused change in offset voltage (V_{OS}) of an op amp an be directly correlated with the design of the input stage; bipolar input op amps having load resistors (as pposed to active current sources) gave the smallest drift in V_{OS}. Theoretical equations have been obtained at qualitatively predict these results. For example, as indicated in Fig. 1, the OP27, OP37, and NE5534 evices have no significant V_{OS} changes; these units all use a bipolar input differential stage with load esistors.

All op amps were evaluated for changes in V_{OS}, input bias current (I_B), power-supply current, open-loop gain (A_{OL}), gain-bandwidth product (GB), slew rate (SR), power-supply rejection ratio (PSRR), and common-mode rejection ratio (CMRR) (see Figs. 2–5).

In general, I_B was the most significant parameter affected by radiation. For bipolar input circuits, the increase in I_B is due primarily to the decrease in h_{FE} of the input transistors; the most significant changes appear in those circuits employing bias current cancellation in the input using pnp lateral transistors. The dielectrically isolated junction field-effect transistor (JFET) input op amp (OPA111) demonstrated the lowest value of I_B (<200 pA) of all op amps tested after a 3 Mrad dose.

Figures 6 and 7 indicate the decrease of open-loop gain A_{OL} with radiation. For most op amps, A_{OL} is still greater than 80 dB after 2 Mrads. Power supply currents of all op amps decreased after irradiations. Devices that gave less than 15% change in supply currents were the OP17, OP27 (PMI), OP37, OPA111, HA2505, HA2525, HA2539, HA2540, HA2625, HA4640, and HA5084. The change in supply current appeared to be a strong function of not only the internal biasing networks used, but also whether the op amp employed dielectric isolation (as do most of the Harris devices) or not. Dielectrically isolated op amps generally had less change in power supply currents than the others. The change that occurs in the gain-bandwidth product with radiation is shown in Figs. 8 and 9. For a typical op amp, the gain-bandwidth product (GB) is related to the input stage transconductance, g_{mI}, and the dominant pole capacitance, C_f, as

$$GB = \frac{g_{mI}}{2\pi C_f} \tag{1}$$

Further, the slew rate (SR) for most general-purpose op amps is determined by the input stage current source I_I and the capacitance C_f, or

$$SR \simeq \frac{I_I}{C_f} = \left(\frac{2\pi I_I}{g_{mI}}\right) GB \tag{2}$$

Since a decrease in power supply current should relate to a decrease in both g_{mI} and I_I, then from Eqs. (1) and (2) the decrease in power supply current should relate correspondingly to a decrease in both GB and SR.

Conclusions

For a general-purpose, low-V_{OS} requirement and in a radiation environment of less than 4 Mrads and 10^{13} n/cm^2, the OP27 and OP37 devices are the best choice of those op amps tested. Unfortunately, the increase in input bias current, I_B, restricts the use of these op amps to circuits that can operate with I_B

changes approaching 0.5 μA; however, the offset current, I_{os}, did remain within 10% of I_B for most units tested. For high-frequency circuits (where changes in I_B are usually not so important), the HA2539–HA2540 op amps should prove useful. Similarly, the other dielectrically isolated units—the HA2505, HA2525, and HA2625—offer low V_{OS} changes, with an I_B increase in all units tested of $\leq 1\ \mu A$. The NE5534, and the NE5532 dual unit, have insignificant V_{OS} changes, but I_B increases to greater than 1 μA. Unfortunately, no field-effect transistor (FET) input op amp tested provided a sufficiently small change in V_{os} to be useful in circuits with dc gains greater than 10. Table 2 summarizes the worst-case changes and categorizes the op amps.

*Research sponsored by the Office of Spent Fuel Management and Reprocessing Systems, performed at Oak Ridge National Laboratory operated by Martin Marietta Energy Systems, Inc., for the U.S. Department of Energy under Contract No. DE-AC05-84OR21400.